AN EXTENDED NICHOLS CHART WITH CONSTANT MAGNITUDE LOCI OF SENSITIVITY AND COMPLEMENTARY SENSITIVITY FUNCTIONS FOR LOOP-SHAPING DESIGN [1]

V. Cerone * **M. Canale** * **D. Regruto** *

* *Dipartimento di Automatica e Informatica, Politecnico di Torino, corso Duca degli Abruzzi 24, 10129 Torino, Italy;* [*vito.cerone, massimo.canale, diego.regruto*]*@polito.it.*

Abstract: Gain and phase margins are widely used stability indices of feedback control systems; although they are both considered explicitly only from the analysis point of view, the phase margin alone is usually considered in the design stage. That is quite restrictive since even if a large phase margin is guaranteed, the feedback control system may show poor robust stability performances. A more general approach consists of bounding the value of the maximum resonance peaks of both the complementary sensitivity and sensitivity functions. In order to handle such resonance peak specifications, it is crucial to set out effective graphical tools which provide explicit reading of closed loop properties from the open loop frequency behaviour. To this end, an Extended Nichols Chart (ENC) which displays constant magnitude loci of the sensitivity function along with the well assessed constant magnitude loci of the complementary sensitivity is introduced in this paper. The advantages of using the ENC in an educational context will be shown in the control design of an unstable laboratory process.

Keywords: Control education, Control system design, Frequency-response methods, Nichols chart, Stability properties.

1. INTRODUCTION

This paper deals with a teaching project on analysis and design of feedback control systems for an undergraduate course in engineering curricula. Analysis and design of single-input, single-output control systems performed through basic Laplace transform techniques and employing standard frequency response tools like Bode, Nyquist and Nichols plots are the topics to be covered in the course. In this context, a feedback cascade compensation scheme, as depicted in Figure 1, is considered.

In such a structure, $G_p(s)$ and $G_c(s)$ are the plant and the controller transfer functions respectively. The bandwidth of the sensor is supposed to be wider than the bandwidth of the control system to be designed, thus in the working frequency range a static gain G_t can be used to describe the sensor behaviour. The static gain G_y is introduced in order to meet desired input-output steady-state gain. The reference signal is

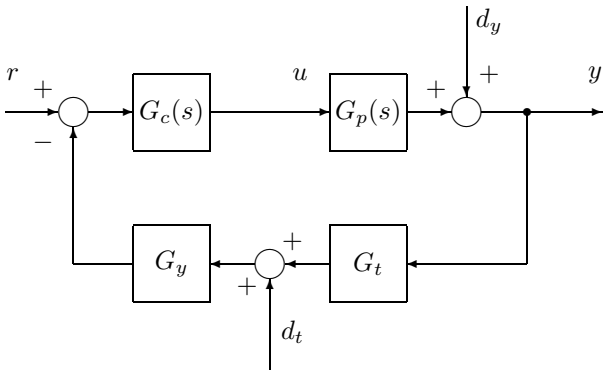

Fig. 1. The considered control structure

r, y is the controlled output and u the control input. Additive output (d_y) and measurement (d_t) disturbances are also considered. The open loop system is denoted by $L(s) = G_c(s)G_p(s)G_tG_y$, the sensitivity function by $S(s) = 1/(1+L(s))$ and the complementary sensitivity function by $T(s) = L(s)/(1+L(s))$.

As to the design procedures to be introduced in the given educational context, loop shaping techniques using standard PID, lag and lead controllers are em-

[1] This research was partly supported by the italian *Ministero dell'Istruzione, dell'Università e della Ricerca (MIUR),* under the plan "Robustness and Optimization techniques for high performance control systems".

ployed. Thus, particular attention has to be devoted to the relationships between the closed loop ($\mid T(j\omega) \mid$ and $\mid S(j\omega) \mid$) and the open loop ($L(j\omega)$) frequency response, which are easily obtained on the Nyquist plane through the use of the constant magnitude loci M_T of $|T(j\omega)|$ (also referred to as the Hall chart) and constant magnitude loci M_S of $|S(j\omega)|$. While the former are part of standard methodologies for frequency domain analysis and design, the latter, to the best of the authors' knowledge, are not considered in classical textbooks for undergraduate course on control system design. Some authors (see, e.g. D'Azzo and Houpis (1995), Kuo and Golnaraghi (2003)) suggests to derive $\mid S(j\omega) \mid$ by drawing the frequency response of the inverse open loop transfer function $1/L(j\omega)$ and using the constant magnitude loci M_T of $|T(j\omega)|$. However, as it requires the drawings of two different plots at one time, this procedure may limit the effectiveness of analysis and design. Besides, polar and/or Nyquist plots representations of the frequency response do not provide an immediate reading of some properties of a given control system such as gain and phase margins. In fact, although both gain and phase margins are naturally defined on the Nyquist plane, they can be directly evaluated on the gain-phase plane through the intersections of the open loop plot with the vertical (-180) and horizontal (0 dB) axes respectively. The gain-phase plane equipped with constant magnitude curves and constant phase curves is the well known Nichols chart. The first educational contribution of this paper, aimed at enhancing and simplifying the use of such analysis and design tool, is to present an extended Nichols chart which displays constant magnitude loci M_S along with the well assessed constant magnitude loci M_T.

In order to show the effectiveness of the presented approach, and to boost its educational aspects, both computer simulation exercises (using MatLab®) and laboratory practice on real processes are included in the course schedule. Laboratory experiments based on real systems are beyond all doubt appealing to students; besides, they are challenging as well since they may show extra features which cannot arise in simulation, even if accurate models are considered. In fact, it is well known that model uncertainty, if not suitably taken into account, may lead to instability or, at the best, to poor performance of the controlled system. However, given the course context, robust analysis and design tools would be far behind the topics of the course, thus suitable indices of stability and/or performance have to be effectively introduced. Indeed, in classical control texts such as Dorf and Bishop (2004), Franklin *et al.* (2002) and Kuo and Golnaraghi (2003), it is remarked the need of taking into account both the gain and phase margins in order to have more realistic measures of the controlled system stability. However, both stability margins are considered explicitly only from the analysis point of view while the phase margin alone is usually considered in the design stage. A more general way to take care of phase and gain margins requirements is to consider both the maximum resonance peaks T_p and S_p of $|T(j\omega)|$ and $|S(j\omega)|$ respectively. The use of the M_T and M_S constant magnitude loci corresponding to T_p and S_p on the Nichols plane allows one to take into account such peak resonance requirements in the shaping of the open loop transfer function frequency response $L(j\omega)$.

While the peak T_p is a standard relative stability measure employed in basic control design, the value of S_p, though introduced in classical textbooks (see Franklin *et al.* (2002)), is not considered in the design procedure. Indeed, since the quantity S_p can be easily related to the maximum plant perturbation that can be added before the closed loop system become unstable (see, e.g. Skogestad and Postlethwaite (1996),Doyle *et al.* (1992)), a requirement on the sensitivity function resonance peak paves the way for the introduction of basic rudiments of robust control in such an undergraduate course. Note that further control design requirements such as low and high frequency disturbances attenuation can be handled considering suitable constant magnitude loci on the Nichols plane. Summarising, the main educational contribution of the paper is the use of the peak S_p, besides T_p, as indices of relative stability through the use of an extended Nichols chart in the loop-shaping approach design of SISO control systems.

2. PROBLEM FORMULATION

Consider the feedback control system of Figure 1, introduced and described in Section 1. The loop, sensitivity and complementary sensitivity transfer functions are defined, respectively, as

$$L(s) = G_c(s)G_p(s)G_tG_y \tag{1}$$

$$S(s) = \frac{1}{1 + L(s)} \tag{2}$$

$$T(s) = \frac{L(s)}{1 + L(s)} \tag{3}$$

The maximum sensitivity S_p and the maximum complementary sensitivity T_p are defined as

$$S_p = \max_{\omega \in [0,\infty]} \mid S(j\omega) \mid \tag{4}$$

$$T_p = \max_{\omega \in [0,\infty]} \mid T(j\omega) \mid \tag{5}$$

Here we address the problem of how to introduce students to the design of feedback control systems in the frequency domain through a loop shaping approach. We deliberately skip the steady-state design and assume that requirements on steady-state polynomial reference tracking and/or polynomial disturbance attenuation/rejection are duly taken into account. It is well known that loop-shaping techniques are employed in the presence of frequency domain specification such as, e.g., sensitivity peak and complementary sensitivity peak requirements, low and/or high

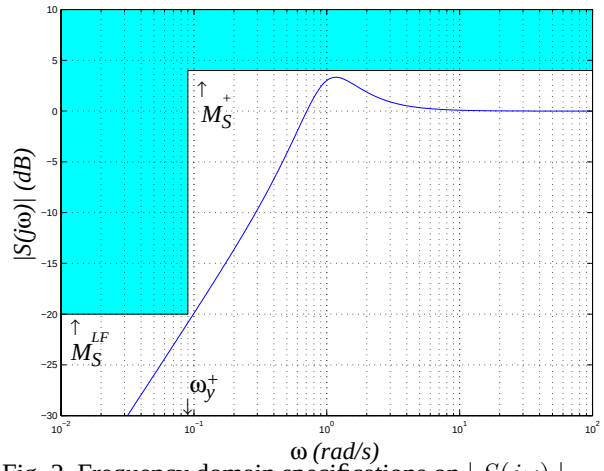

Fig. 2. Frequency domain specifications on $\mid S(j\omega) \mid$.

frequency disturbance attenuation, bandwidth, etc.. As up-to-date instructors may know, frequency domain control systems design methods reported in classical undergraduate textbooks (see the list of references) are based on phase margin (*PM*) and gain margin (*GM*) specifications, which, usually are chosen on the basis of the designer's experience. Besides, in almost all the books in the lists of references, lower bounds on *PM* and *GM* are derived in terms of T_p, while only in a couple of textbooks (see e.g. Wolovich (1994),Skogestad and Postlethwaite (1996)) lower bounds on *PM* and *GM* are derived in terms of T_p and S_p. In practice, however, only *PM* requirements are usually considered, while *GM* specs are almost entirely ignored and, unfortunately, even if conditions on *GM* and *PM* are fulfilled, satisfaction of desired given performance on T_p and S_p is not guaranteed. In this paper we present a frequency domain design approach based on loop shaping subject to the following constraints

$$S_p \leq M_S^+ \tag{6}$$

$$T_p \leq M_T^+ \tag{7}$$

where $M_S^+ > 1$ and $M_T^+ > 1$ are upper bounds on sensitivity peak S_p and complementary sensitivity peak T_p respectively. Both S_p and T_p can be obtained from frequency domain specifications on $S(j\omega)$ and $T(j\omega)$ which, for example, may have the shape shown in Figure 2 and Figure 3 respectively. If frequency disturbance attenuation requirements are specified, further constraints can be added to the loop shaping problem. Indeed, if

$$d_y = a_y \sin \omega_y t \qquad \forall \omega_y \leq \omega_y^+ \tag{8}$$

where ω_y^+ and a_y are given, and the output error due to d_y is required to be bounded by a given ρ_y, then it is easy to see that the following constraint on $S(j\omega)$ can be derived

$$|S(j\omega_y)| \leq \frac{\rho_y}{a_y} \doteq M_S^{LF} \qquad \forall \omega_y \leq \omega_y^+ \tag{9}$$

where M_S^{LF} is the required low frequency attenuation level (see Fig. 2). While, if

$$d_t = a_t \sin \omega_t t \qquad \forall \omega_t \geq \omega_t^- \tag{10}$$

where ω_t^-, and a_t are given, and the output error due to d_t is required to be bounded by a given ρ_t, then it is easy to see that the following constraint on $\mid T(j\omega) \mid$ applies

$$|T(j\omega_t)| \leq \frac{\rho_t}{a_t} \doteq M_T^{HF} \qquad \forall \omega_t \geq \omega_t^- \tag{11}$$

where M_T^{HF} is the required high frequency attenuation level (see Fig. 3).

As remarked in a couple of textbooks taken from the literature (Wolovich (1994),Franklin *et al.* (2002)), although *PM* and *GM* are considered as classical measure of relative stability of nominal systems, they may fail to guarantee a reasonable bound on the distance of the loop transfer function $L(j\omega)$ from the critical point $(-1, 0)$ on the Nyquist plane. On the contrary, S_p, the maximum of $|S(j\omega)|$, can be successfully used to obtain simple bounds on both the phase margin and the gain margin. In other words, a single bound on S_p can be employed as a measure of robust stability in all closed loop stable systems, including the nonminimum phase and open-loop unstable cases in which both the *PM* and the *GM* are ill-defined. As a matter of fact, the maximum sensitivity S_p is the inverse of the shortest distance from the Nyquist plot of $L(j\omega)$ to the critical point $(-1, 0)$ on the complex plane, thus it must be stressed that constraint (6) can ensure stability robustness of the closed loop system subject to plant modeling uncertainty. Furthermore, although not so obvious, constraint (7) provides robust stability as well when the plant is affected by multiplicative uncertainty (Skogestad and Postlethwaite (1996)).

Remark — The approach proposed in this work can be seen as a special case of the quantitative feedback design theory (QFT) which is an advanced methodology for dealing with plant uncertainty (see Horowitz (1993)). Indeed, given the plant templates, QFT converts closed-loop magnitude specifications (such as, e.g., (6), (7), (9), (11)) into magnitude and phase constraints on a nominal open-loop function. These constraints are called QFT bounds. However, Horowitz's approach is much too advanced to be introduced to undergraduate students.

3. THE NICHOLS CHART REVISITED AND EXTENDED

If we set $L(j\omega) = X + jY$, it is well known that the loci of constant $\mid T(j\omega) \mid = M_T$ in the Nyquist plane are the circles given by

$$Y^2 + \left(X + \frac{M_T^2}{M_T^2 - 1} \right)^2 = \frac{M_T^2}{(M_T^2 - 1)^2} \tag{12}$$

which are also called M_T-circles. To the best knowledge of the authors, the locus of points corresponding to constant-$\mid S \mid$ is not considered in any of the undergraduate textbooks we had to hand. It is a bit less

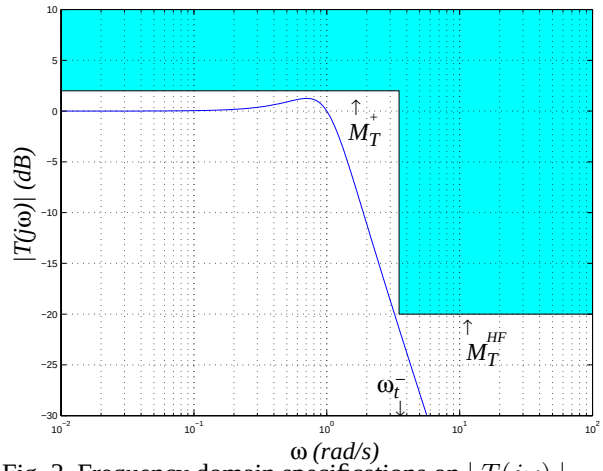

Fig. 3. Frequency domain specifications on $|\ T(j\omega)\ |$.

involved of the constant-$|\ T\ |$ circles and is a circle given by

$$Y^2 + (X+1)^2 = \frac{1}{M_S^2} \tag{13}$$

Constant-$|\ S\ |$ circles can be successfully used for analysis and design the same way constant-$|\ T\ |$ circles are. We emphasize that setting upper bounds on T_p and S_p is equivalent to draw a couple of "forbidden" circles, around the critical point $(-1, 0)$, inside which $L(j\omega)$ is not allowed to lie. Constant magnitude and/or phase circles are easily understood in the complex plane where polar and Nyquist plots are usually drawn. However, constant magnitude contours can also be plotted on the gain-phase plane which displays the gain (in decibels) versus the phase (in degrees) readily available from Bode plots. A major disadvantage in working in the polar coordinates plane with the Nyquist plot of $L(j\omega)$ is that the curve no longer retains its original shape when simple modifications on the loop gain are made. For example, when the static loop gain is modified, the $L(j\omega)$ curve is shifted upwards or downwards in the vertical direction without distortion. In the gain-phase plane, the contours are no longer circles. Such constant magnitude contours together with constant phase contours of $T(j\omega)$ are referred to as a *Nichols chart*. From a Nichols chart and a gain-phase plot of $L(j\omega)$, one can read, for any frequency point, the magnitude and phase of $T(j\omega)$. In particular, one can easily evaluate the peak value of $|T(j\omega)|$. In some textbooks, see e.g. Kuo and Golnaraghi (2003), it is suggested that the Bode plot of $|S(j\omega)|$ can be derived from the Nichols chart by plotting the locus of $L^{-1}(j\omega)$ rather than $L(j\omega)$ and using constant-$|\ T\ |$ curves. However, in the authors' experience that procedure is rather too involved since one must draw both the direct and the inverse plot of $L(j\omega)$. Instead, in this paper we propose to use constant-$|\ S\ |$ curves beside well known constant-$|\ T\ |$ curves on the gain-phase plane, which will be referred to the *Extended Nichols Chart* (*ENC*). We suggest to use the *ENC* with (a) one constant-$|T|$ curve with level M_T^+, (b) one constant-$|\ S\ |$ curve with level M_S^+, (c) one constant-$|T|$ curve with level M_T^{HF} which takes into account a possible requirement on high frequency disturbance attenuation (if any) and (d) one constant-$|\ S\ |$ curve with level M_S^{LF} which takes into account a possible requirement on low frequency disturbance attenuation (if any). Figure 4 shows a possibile *ENC* with $M_T^+ = 1.23$, $M_S^+ = 1.54$, $M_T^{HF} = 0.1 \equiv -20$ dB and $M_S^{LF} = 0.1 \equiv -20$ dB.

4. CONTROLLER DESIGN FOR A REAL LABORATORY PROCESS USING THE *ENC*

In this section the design of a controller for a laboratory magnetic ball levitation system is considered in order to show the use and the effectiveness of the *ENC*. The main purpose here is to highlight that the *ENC* allows students to design robust and effective controllers for a real plant by means of basic loop shaping techniques. As well known ((Oliveira and Costa, 1999; Shiakolas and Piyabongkarn, 2003; Galvão *et al.*, 2003)) the magnetic levitation system is inherently nonlinear and unstable, thus the control of such a system is not a trivial problem, especially for inexperienced undergraduate students. For a detailed description of the considered levitation system the reader is referred to the book Greco *et al.* (2003) and the Internet Web page *www.ladispe.polito.it/it/html/levitatore.htm* (n.d.). A standard Intel® Celeron® 500 computer equipped with the MATLAB® Real Time Workshop® is used for the implementation of the controller with a sampling time $T_s = 0.001$ s.
The following approximated linear model of the system has been obtained through linearization around a suitable operating point (u^o, y^o):

$$G_p(s) = \frac{-15.34}{(s - 30.34)(s + 30.34)} \tag{14}$$

$$G_t = 555.89 \text{ V/m} \tag{15}$$

where, with reference to the block diagram of Figure 1, $G_p(s)$ is the transfer function from the voltage command $u(t)$ to the the ball position $y(t)$, G_t is the static gain describing the optical transducer and $G_y = 1$ which implies that the input-output static gain equals $1/G_t$. The students are required to design a digital filter in order to control the position of the suspended ball around the operating point. More precisely, the closed loop system has to satisfy the following tracking performance specifications when the reference signal $r(t)$ is a zero-mean valued square wave with period $T_r = 4$s, duty cycle 50% and amplitude $r_a = 0.1$ V which corresponds to a ball displacement of about 0.18 mm around the operating point:

- (S1) zero steady-state error;
- (S2) rise time $t_r \leq 0.015$ s;
- (S3) overshoot $\hat{s} \leq 25\%$.

In order to exploit frequency domain techniques for the controller design, we have to translate the time domain specifications (S1) – (S3) into suitable frequency

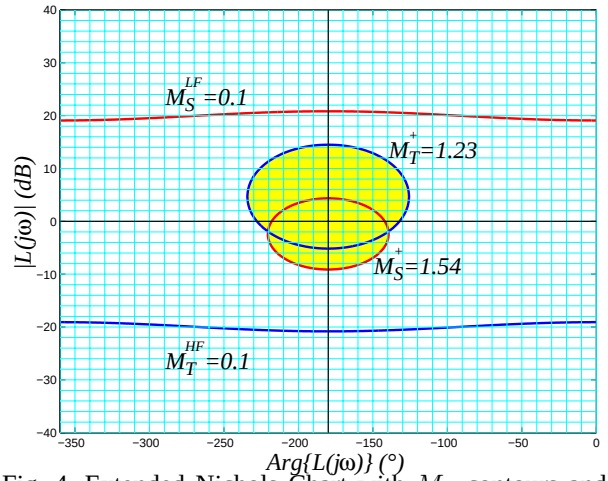

Fig. 4. Extended Nichols Chart with M_T-contours and M_S-contours.

domain constraints. As well known, specification (S1) simply requires an integrator in the controller in order to get a type I control system. As far as specifications (S2) and (S3) are concerned, relations between time domain and frequency domain response of prototype second order systems can be exploited to get the following bounds on the cross-over frequency ω_c and the closed loop peaks T_p and S_p:

$$\omega_c > \omega_c^- = 120 \text{ rad/s} \tag{16}$$

$$T_p < M_T^+ = 1.35 \text{ (2.6 dB)} \tag{17}$$

$$S_p < M_S^+ = 1.65 \text{ (4.35 dB)} \tag{18}$$

The *ENC* with $M_T^+ = 1.35$ and $M_S^+ = 1.65$ is shown in Figure 5. The following controller with three lead networks has been designed to satisfy inequality (16) and the constraints on the *ENC* defined by the constant-$|\ T\ |$ curve with level M_T^+ and the constant-$|\ S\ |$ curve with level M_S^+:

$$C_{ENC}(s) = \frac{-19(s/30+1)^2(s/400+1)}{s(s/3200+1)(s/900+1)^2} \tag{19}$$

The digital loop transfer function $L_{ENC}(z)$, provides a cross-over frequency $\omega_c \approx 209$ rad/s and satisfies the constraints on the *ENC* as shown in Figure 5.

In order to show the educational benefits of the use of the *ENC*, $C_{ENC}(s)$ is compared with a controller designed exploiting the classical approach based on gain and phase margins specifications. To this end the following relations (Wolovich (1994), Skogestad and Postlethwaite (1996)) can be used to obtain lower bounds on the gain and phase margins from (17) and (18): $GM > GM^+$ and $PM > PM^+$, where

$$GM^+ = \max\left\{\frac{S_p}{S_p-1}\ ,\ 1+\frac{1}{T_p}\right\} = 2.54 \text{ (8 dB)} \tag{20}$$

$$PM^+ = \max\left\{2\arcsin\frac{1}{2S_p}\ ,\ 2\arcsin\frac{1}{2T_p}\right\} = 43.5^o. \tag{21}$$

The following controller with three lead networks has been designed to satisfy inequalities (16), (20) and (21):

$$C_{mrg}(s) = \frac{-40(s/75+1)^3}{s(s/525+1)^3} \tag{22}$$

The digital loop transfer function $L_{mrg}(z)$, provides a cross-over frequency $\omega_c \approx 155$ rad/s, a gain margin $GM \simeq 8.3$ dB and a phase margin $PM \simeq 44^o$ as shown in Figure 5.

The frequency responses of the complementary sensitivity and the sensitivity functions obtained with the controllers C_{ENC} and C_{mrg} and computed on the basis of the approximated linear model $G_p(s)$ are shown in Figure 6. As expected, the closed loop control system obtained with the controller C_{ENC} satisfies the frequency domain performance specifications on the peaks of $|S(j\omega)|$ and $|T(j\omega)|$ while that is not the case for the closed loop system obtained with the controller C_{mrg}.

The experimental square wave responses obtained with the controllers C_{ENC} and C_{mrg} are shown in Figure 7. As can be seen, both the closed loop systems do not satisfy the performance specification (S3) on the overshoot; that is due to: (i) the fact that the relations used to map time domain specification (S1) – (S3) into the frequency domain constraints (16), (17) and (18) are exact only for prototype second order systems while the obtained closed loop systems is not a prototype second order systems; (ii) the effect of the mismatch between the approximated linear model used for the design of the controllers and the complex nonlinear dynamics of the real plant. However, it can be noted that, in spite of i) and ii), the controller designed on the basis of the *ENC* guarantees a worst case maximum overshoot $\hat{s} \approx 32.4\%$; on the contrary the response of the closed loop systems obtained with the controller C_{mrg} shows lightly damped oscillations and a worst case maximum overshoot $\hat{s} = 108\%$.

5. DISCUSSION AND CONCLUSION

In the example of Section 4, we have compared, on a real plant, the performance of the controller C_{ENC}, designed using the proposed *ENC*, with a controller C_{mrg} which satisfies the gain and phase margin constraints. Actually, the controller C_{mrg} leads to a bad-shaped loop transfer function and an experienced control engineer would avoid such a pathological controller even without the use of the *ENC* but that could not be the case when the design has to be performed by an undergraduate student. The aim of the presented example is twofold. Firstly we notice that the classical frequency domain design approach, based on gain and phase margin requirements, can lead to closed-loop systems which do not satisfy typical frequency domain performance specifications on $|S(j\omega)|$ and $|T(j\omega)|$ of the kind shown in Figure 2 and Figure 3; besides such a design method may also fail to guarantee good robustness properties. Secondly, we have shown that the *ENC* is a simple and effective tool to fulfill performance specifications expressed in terms of constraints on the frequency response of S and T. Besides, trying to avoid the "forbidden region" delimited by the constant-$|T|$ curve with level M_T^+ and the constant-$|S|$

curve with level M_S^+, the student is guided through the design of an inherently robust controller.

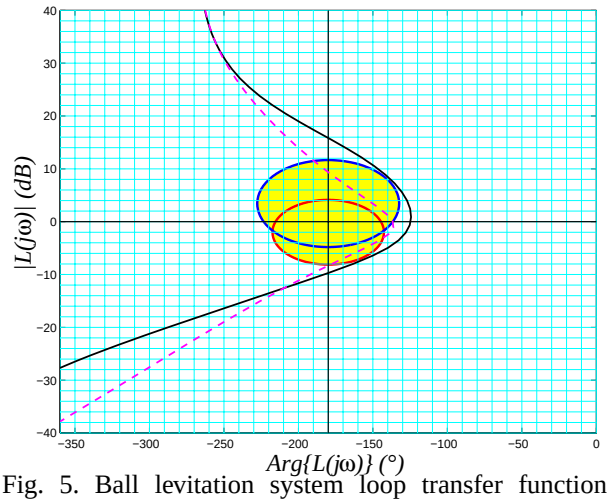

Fig. 5. Ball levitation system loop transfer function plot on the ENC: C_{ENC} (black-solid) and C_{mrg} (magenta-dashed).

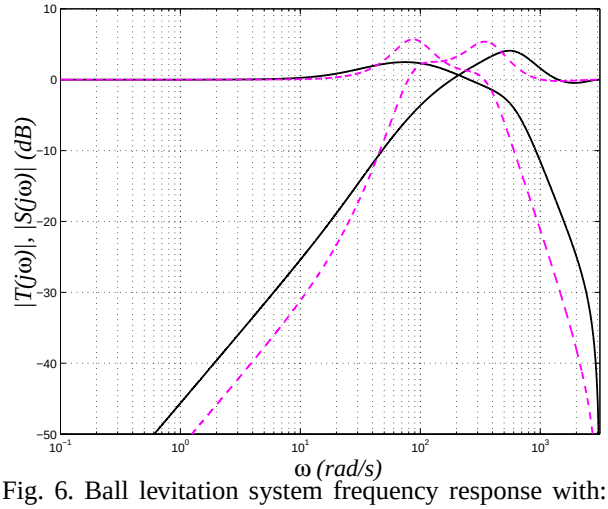

Fig. 6. Ball levitation system frequency response with: C_{ENC} (black-solid) and C_{mrg} (magenta-dashed).

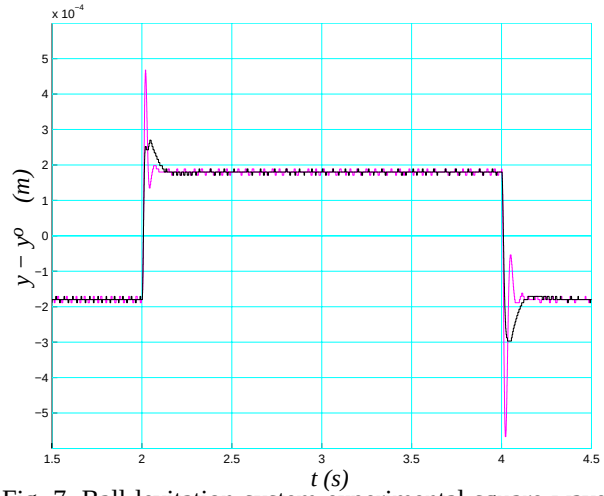

Fig. 7. Ball levitation system experimental square wave response with: C_{ENC} (black-thick) and C_{mrg} (magenta-thin).

REFERENCES

Chen, C. T. (1993). *Control System Design*. Saunders College Publishing. Orlando, Florida.

D'Azzo, J. J. and C. H. Houpis (1995). *Linear control system analysis and design: conventional and modern*. 4^{th} ed.. McGraw–Hill. New York.

de Vegte, J. Van (1994). *Feedback Control Systems*. 3^{rd} ed.. Prentice–Hall. Englewood Cliffs, New Jersey.

Dorf, R. C. and R. H. Bishop (2004). *Modern Control Systems*. 10^{th} ed.. Prentice–Hall. Upper Saddle River, New Jersey.

Doyle, J. C., B. A. Francis and A. R. Tannenbaum (1992). *Feedback Control Theory*. Macmillan Publishing Company. New York.

Dutton, G., S. Thompson and B. Barraclough (1997). *The Art of Control Engineering*. Addison Wesley Longman.

Franklin, G. F., J. D. Powell and A. Emami-Naeini (2002). *Feedback Control of Dynamic Systems*. 4^{th} ed.. Macmillan Publishing Company. New Jersey.

Galvão, R. K. H., T. Yoneyama, F. M. Ugolino de Araújo and R. G Machado (2003). A simple technique for identifying a linearized model for a didactic magnetic levitation system. *IEEE Trans. on Education* **46**(1), 22–25.

Goodwin, G. C., S. F. Graebe and M. E. Salgado (2001). *Control System Design*. Prentice–Hall. Upper Saddle River, New Jersey.

Greco, C., M. Rulla and L. Spagnolo (2003). *Laboratorio sperimentale di automatica*. McGraw-Hill Italia. Milano, Italy.

Horowitz, I.M. (1993). *Quantitative feedback theory*. QFT Publications. Boulder, Colorado.

Kuo, B. J. and F. Golnaraghi (2003). *Automatic Control Systems*. 8^{th} ed.. John Wiley & Sons. New York.

Lewis, P. H. and C. Yang (1997). *Basic Control Systems Engineering*. Prentice–Hall. Upper Saddle River, New Jersey.

Nise, N. S. (2004). *Control Systems Engineering*. 4^{th} ed.. John Wiley & Sons. New York.

Ogata, K. (1997). *Modern Control Engineering*. 3^{rd} ed.. Prentice–Hall. Upper Saddle River, New Jersey.

Oliveira, V. A. and E. F. Costa (1999). Digital implementation of magnetic suspension control system for laboratory experiments. *IEEE Trans. on Education* **42**(4), 315–322.

Phillips, C. L. and R. D. Harbor (2000). *Feedback Control of Dynamic Systems*. 4^{th} ed.. Prentice–Hall. Upper Saddle River, New Jersey.

Rohrs, C. E., J. L. Melsa and D. G. Schultz (1993). *Linear Control Systems*. McGraw–Hill. New York.

Shiakolas, P. S. and D. Piyabongkarn (2003). Development of a real-time digital control system with hardware-in-the-loop magnetic levitation device for reinforcement of controls education. *IEEE Trans. on Education* **46**(1), 79–87.

Skogestad, S. and I. Postlethwaite (1996). *Multivariable Feedback Control*. 1^{st} ed.. John Wiley & Sons. New York.

Stefani, R. T., B. Shahian, C. J. Savant Jr. and G. H. Hostetter (2002). *Design of Feedback Control Systems*. 4^{th} ed.. Oxford University Press. New York.

Stefano, J. J. Di, A. R. Stubberud and I. J. Williams (1990). *Feedback and Control Systems*. 2^{th} ed.. McGrawHill. New York.

Wolovich, W. A. (1994). *Automatic Control*. Saunders College Publishing. Orlando, Florida.

www.ladispe.polito.it/it/html/levitatore.htm (n.d.).